Gamma-spectroscopy-based survey of the devices on a board activated by proton beams from the K150 cyclotron

V. Horvat

Devices on a board shown in Fig. 1 have been irradiated by proton beams from the K150 cyclotron. As a result, the devices (and parts of the board) have been activated above the background level, and the induced activity had to be analyzed before the board with the devices could be returned to the owner.

Fig. 1. Devices on a board irradiated by proton beams from the K150 cyclotron.

The survey was performed using an apparatus purchased from Berkeley Nucleonics Corporation (BNC) [1]. It includes a lanthanum bromochloride (LBC) scintillation detector with a 2" diam. x 2" thick crystal, coupled to a photomultiplier tube (PMT) [3, 4]. The tube is plugged into the socket of a PMT base

integrated with an amplifier, an analog-to-digital converter, and a multichannel analyzer (MCA) [5]. The data acquisition and analysis software [6] and a personal computer were purchased separately. The crystal and the PMT are encapsulated in 0.4 mm thick aluminum to protect the detector from ambient light and moisture and to reflect the scintillation light. The new apparatus has been well characterized in terms of its intrinsic background, efficiency, energy scale, and resolution as a function of energy.

Measurements and subsequent analysis were challenging because of the large size (9.5" x 7.5") and complicated (non-planar) geometry of the board and the devices on it. Ideally, the board should be measured from a distance much larger than the 30 cm length of its diagonal, so that the board could be regarded as a point-like source. However, this is neither practical (because there is not enough room in the lab for that) nor feasible. Namely, the maximum detector counting rate at the surface of the board is less than four times that of the background, and so at a large distance the contribution from the board is surely well below the background level and therefore not detectable.

Consequently, we opted to measure the activity at a distance of 30 cm from the board, as shown in Fig. 1, hoping to determine intensity of the strongest peak in the spectrum with good accuracy (on the order of a few percent). This is also justified by the fact that the detector solid angle is large (more than 2π). As a follow-up, we measured activity at the surface of each device in order to determine intensities of the weaker peaks relative to the strongest one and use that information to identify the active nuclides and their relative activities. Each measurement involving the board was immediately followed by a background measurement in the same configuration. Spectra measured at the distance of 30 cm are shown

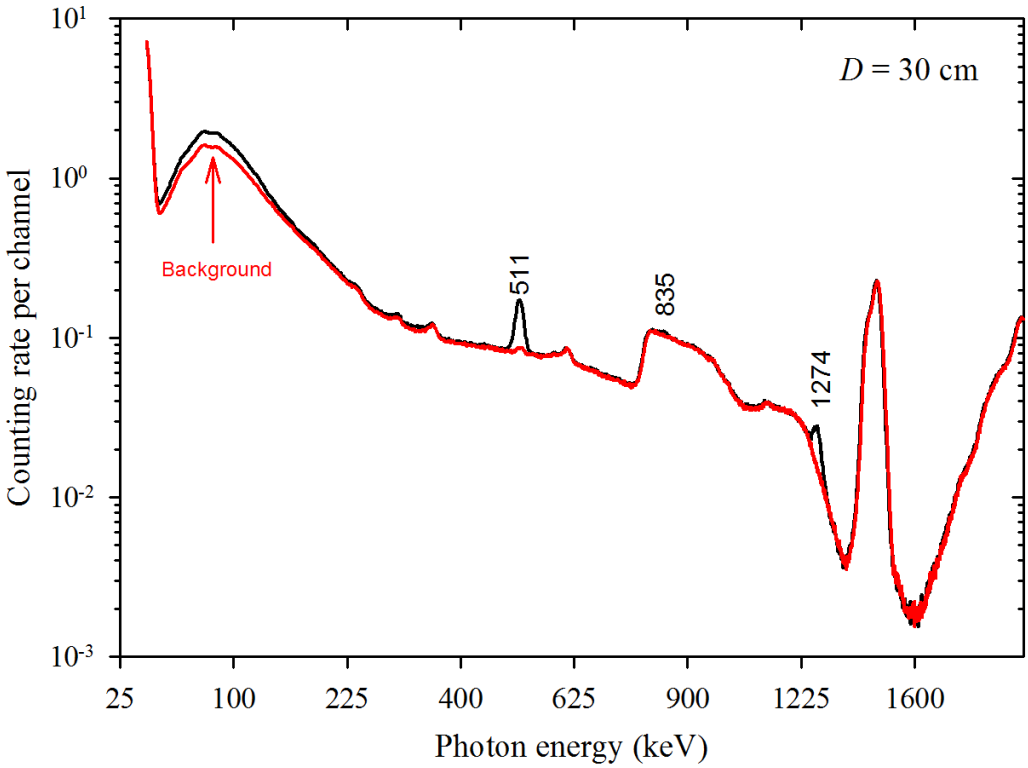

Fig. 2. Photon spectrum of the board taken at the distance of 30 cm (shown in black) and the corresponding background spectrum (shown in red).

in Fig. 2, while some of the spectra measured at the surfaces of the devices are shown in Fig. 3.

Fig. 2 shows very few peaks discernible above the background level, although there may be additional peaks in the regions where the background is high. The peak at 1274 keV is characteristic of Na-22 decay, as is the peak at 511 keV due to annihilation of the positrons emitted in the process. The peak at 835 keV is characteristic of Mn-54 decay. The structure between 789 keV and 1044 keV, the peaks at about 1450 keV, as well as the structure above 1600 keV are all attributed to the intrinsic background of the LBC detector [7-10]. The broad distribution centered at about 85 keV is due to the x-ray emissions from the nearby ECR sources. Intensity of that distribution varies over time depending on the source usage. Unfortunately, it was not practical to shield the detector from these x rays when the detector was 30 cm above the board. However, this was done very effectively for the subsequent measurements in which the detector was close to the board, by building a lead-brick structure around the setup. The small peaks that show up in both spectra shown in Fig. 2 are environmental, mostly due to radon and its descendants. Their intensity also varies over time.

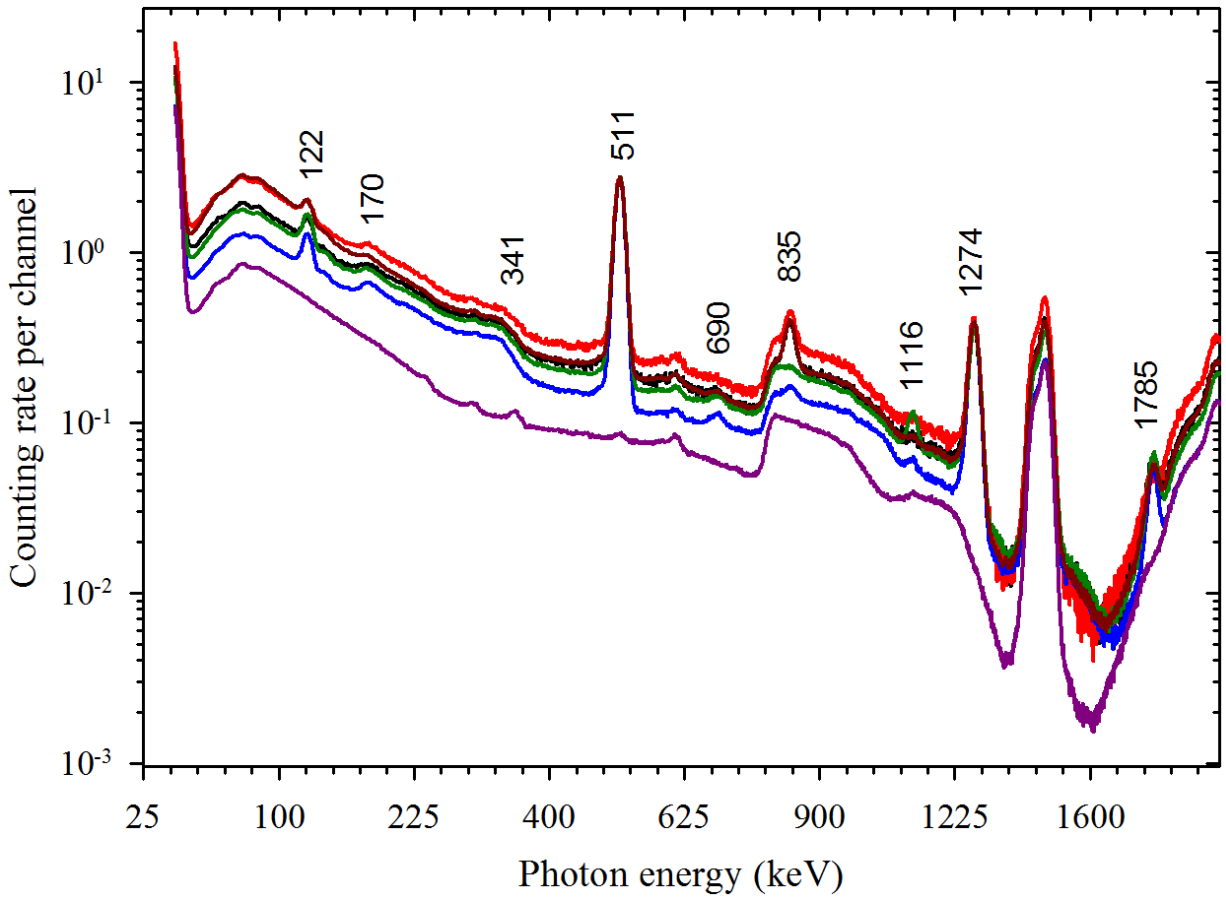

Fig. 3. Selected photon spectra measured at the surfaces of the devices, slightly renormalized to match the amplitude of the 511 keV peak in the spectrum shown in blue. The remaining measured spectra do not display any new features. The corresponding background spectrum is shown in purple.

Fig. 3 shows selected photon spectra measured at the surfaces of the devices. Compared to Fig. 2, new peaks have emerged due to the more favorable peak-to-background ratio and the increased counting rate. The ridges at 170 keV and 340 keV represent edges of the 511 keV peak's Compton distribution,

while the peak at 1785 keV is due to coincidence summing (511 keV + 1274 keV). The remaining three new peaks are at 122 keV (characteristic of Co-57 decay), at 1116 keV (characteristic of Zn-65 decay), and at 690 keV. Origin of the peak at 690 keV is not clear, but since the peak is very weak (comparable in intensity to the nearby environmental peak), its contribution to the overall activity of the sample can be ignored.

It should be noted that the spectra shown in Figs. 2 and 3 were measured about seven months after exposure of the board to the proton beam. Consequently, all the short-lived activity had decayed away, and the nuclides with half-lives on the order of one hundred days or more do not emit gamma rays outside of the energy region shown in the graphs. A few spectra were taken with photon energy range extended up to 3000 keV to confirm that assertion for the case at hand.

Peaks in the spectra were analyzed using bGamma software[11-12] that featured a National Nuclear Data Center (NNDC) photon-emission database NuDat [13-14], while the efficiency at the distance of 30 cm from the board was calculated using CYLTRAN, a Monte Carlo electron-and-photon transport code [15]. CYLTRAN was verified to produce accurate efficiency values in the previous measurements featuring various calibrated gamma-ray sources located at different distances from the detector and at different displacements from the detector axis. Unfortunately, the complex geometry of the board and the devices on it could not be modeled precisely in CYLTRAN. Therefore, we simplified the model to reflect the worst-case scenario (*i.e.*, the lowest possible efficiency). Two configurations were considered. In one configuration the board was modeled as a thin disc having diameter of 30 cm and having its radioactivity uniformly distributed on its surface. In the other configuration board was modeled as a thin disc having diameter of 1 cm and having its radioactivity uniformly distributed on its surface, but unlike in the previous case, it was displaced away from the detector axis, by as much as 14 cm. As expected, the efficiency turned out to be lower in the latter case and that set of values was used in the analysis. Nevertheless, the differences between the two sets of efficiencies were reassuringly small, ranging from 1.6% at 122 keV up to 6.3% at 1274 keV.

Analysis showed that the emission at 511 keV is almost entirely due to Na-22 decay and that the upper limit of activity associated with the peak at 691 keV is only 50 ± 8 decays per second (dps) or 1.3 ± 0.2 nCi and can be ignored. The report summary is presented in Table I below.

Table I. Activity of the nuclides from the board.

Nuclide	Half-life	Activity (dps)	Activity (nCi)
Na-22	2.60 y	1438 ± 26	38.8 ± 0.7
Mn-54	312 d	355 ± 6	9.6 ± 0.2
Zn-65	244 d	251 ± 8	6.8 ± 0.2
Co-57	272 d	133 ± 2	3.60 ± 0.06

[1] https://www.berkeleynucleonics.com
[2] https://cyclotron.tamu.edu/see/
[3] https://www.berkeleynucleonics.com/lanthanum-bromochloride
[4] https://scionix.nl/high-resolution-lbc-scintillators/

[5] https://www.berkeleynucleonics.com/bmca-ethernet
[6] https://www.berkeleynucleonics.com/bgamma-software-package
[7] S. Petrak, M. Selle, P. Schotanus, E. Bodewits, and F. Quarati, Scintillation Properties of high-resolution $La(Br_x\ Cl_{1-x})_3$:Ce and high-sensitivity CeBr3, 14^{th} Int. Conference on Scintillating Materials and their Applications (SCINT), Chamonix, France, 2017.
[8] F. Quarati *et al*., Nucl. Instrum. Methods Phys. Res. **A729**, 596 (2013).
[9] G. Hull *et al.*, Nucl. Instrum. Methods Phys. Res. **A925**, 70 (2019).
[10] J.K. Hartwell and R.J. Gehrke, Applied Radiation and Isotopes **63**, 223 (2005).
[11] http://www.brightspec.be/brightspec/index.php
[12] https://www.brightspec.be/brightspec/?q=node/42
[13] N. D. C. National, "NuDat V2," Brookhaven National Laboratory, USA, 2018.
[14] N. N. D. Center, " http://www.nndc.bnl.gov/nudat2/," BNL. [Online]. [Accessed Nov 2018].
[15] J.A. Halbleib and T.A. Mehlhorn, Nucl. Sci. Eng. 92, 338 (1986), J.A. Halbleib, R.P. Kensek, T.A. Mehlhorn, G.D. Valdez, S.M. Seltzer, and M.J. Berger, CYLTRAN 3.0, Sandia National Labs (Albuquerque, NM), Report SAND91-1634 (1992).